Journal of Chemical Health Risks

Journal of Chemical Health Risks (2017) 7(1), 19–32

ORIGINAL ARTICLE

Study of Methyl *tert*-butyl Ether (MTBE) Photocatalytic Degradation with UV/TiO_2-ZnO-CuO Nanoparticles

Mohsen Mansouri[*1], Mohsen Nademi[2], Mohammad Ebrahim Olya[3], Hossein Lotfi[2, 3]

[1] Department of Chemical Engineering, Ilam University, Ilam, Iran

[2] Department of Chemical Engineering, North Tehran Branch, Islamic Azad University, Tehran, Iran

[3] Department of Environmental Research, Institute for Color Science and Technology, Tehran, Iran

(Received: 14 July 2016 Accepted: 17 September 2016)

KEYWORDS

Photocatalytic degradation;
MTBE;
TiO_2 – ZnO - CuO nanoparticles;
Response surface modeling

ABSTRACT: In this study, the TiO_2-ZnO-CuO nanoparticles were primed by sol-gel method characterized by X-ray diffraction (XRD) and Scanning Electron Microscopy (SEM), for degradation of MTBE solution in water. The effectiveness of the treatment method applied for the degradation of MTBE based on an advanced photocatalytic oxidation process was investigated. The three various key parameters were optimized using response surface modeling namely: pH, TiO_2-ZnO-CuO concentration and the initial MTBE concentrations. The optimized values were obtained at the PH (7), TiO_2-ZnO-CuO concentration (1.49 g/L), and the initial MTBE concentration (31.46 mg/L). Finally, kinetics reaction of degradtion MTBE was carried in the optimum conditions.

INTRODUCTION

Methyl tertiary-butyl ether (MTBE) has been classified by the united states environmental protection agency (USEPA) as a conceivable carcinogenic agent. Based on this agancy standards, the allowablerestriction of MTBE in drinking water is 20-40 ppb [1-3]. This limitation prevented its use as a gasoline additive since May 2006 [4].

The paramount characteristics of this oxygenated material are high polarity and low Henry constant coefficient of 0.022 [5]. In addition, without being absorbed in the soil, this substance can easily penetrate to the ground, and cause groundwater contamination. Besides, MTBE could be easily evaporated to the air and then return back into the aquatic environment via precipitation. MTBE is identified as a very resistant substance for the natural environmental degradation becauseof existence of ether bond and long sub branches (more than one carbon) in its structure [6].

MTBE is a semi volatile organic compound, has been extensively used as a gasoline additive for improved oxidation. In the last decade, its distribution in the aquatic environment and its occurrence in drinking water resources has become a major issue in the

* Corresponding author: mansouri2010@yahoo.com; m.mansouri@ilam.ac.ir (M. Mansouri).

United States and in Europe [7, 8]. The main sources of MTBE contamination in the environment are leaking underground storage tanks, exhausts from recreational watercrafts, urban runoff and air deposition [8, 9]. MTBE has a high vapor pressure, which predicts volatilization from soil surfaces. "However, its high water solubility, small molecular size and relatively low Henry's law constant imply that its solution predominates its volatilization. In addition, MTBE is very mobile in the soil solution and hardly sorbs to soil particles" [10].

Recently, many technologies have been used for MTBE degradation in water. Some of them comprised granular activated carbon (GAC), adsorption, air stripping, advance oxidation processes (AOPs) and biodegradation [11].

One of the efficient techniques for the removal of organic dyes is advanced oxidation processes (AOP) using heterogeneous semiconductor photocatalysts in which the hydroxyl radicals (OH) are the main oxidizing regents for the photocatalytic decolorization of Azo dyes [12-14]. AOPs involve chemical, photochemical or electrochemical processes leading to chemical degradation of organic pollutants. Among the semiconductors used in AOPs, TiO_2 and ZnO has been successfully applied as a photocatalyst for decolorization of dye pollutants [15,16].

Titanium dioxide (TiO_2) is one of the most common catalysit which was widespreadly applied for photocatalytic degradation of organic contaminants in water and air because of unique features like its high photocatalytic actvity, non-soluble, non-toxic, and low prodauction cost, but one of the major problems in applicationof pure TiO_2 is recombination between electron and hole. Several studies such as metal or nonmetal iron doping were accomplished to pave the way for ameliorating photocatalytic efficacy of TiO_2 [17-21].

In this study, the sol-gel method was used to synthesize TiO_2-ZnO-CuO nanoparticles. Then, characterizations of prepared TiO_2-ZnO-CuO nanoparticles were characterized by X-ray diffraction (XRD), and scanning electron microscope (SEM). After this procedure, the effects of different workable parameters such as solution's initial pH, TiO_2-ZnO-CuO and contaminant's concentration on photocatalytic degradation of MTBE were tested. Finally, the optimal conditions were obtained through the experiments.

MATERIALS AND METHODS

Materials

For the purpose of synthesis, hydroxyl propyl cellulose (HPC), titanium tetraisopropoxide (TTIP), acetic acid, pure alcohol, $Zn(NO_3)_2.6H_2O$, di-ethanol amine, ethanol amine, $Cu(NO_3)_2.6H_2O$, NaOH, H_2SO_4, and Methyl *tert*-butyl ether (99.9 %)– all in analytical grade – were purchased from Merck Company.

Instruments

To determine nanoparticles' structure, XRD (Philips PW 1800) was employed. Scanning electron microscope (SEM) (Leo 1455 VP) was used to identify the nanoparticles' surface morphology. The MTBE concentrations were measured with UV-Vis spectrophotometer (Model $T80^+$, PG Instruments, and UK) device. The gas choromatography was equipped with a helium ionization detector (HID) (Model GC-Acme 6100, Korea). A TRB-5 quartz capillary column of (30 m × 0.53 mm) with a 3-µm film thickness was used in UV-Vis spectrophotometer.

Preparation of nanocatalyist

For synthesis of TiO_2-ZnO-CuO nanocomposite, each part of it should be prepared separately before mixing by sol-gel method. Afterwards, the method of constructing of each component of nanocomposite will explain.

For preparing of TiO_2, at the first, hydroxyl propyl cellulose (HPC) was solved in ethanol under quick stirring for five minutes. Then, titanium tetraisopropoxide (TTIP) was added to previous mixture

and was stirred for fifteen min. After that, the mixture of glacial acetic acid, pure alcohol and deionized water was added to previous mixture. It was stirred for fifteen minutes just to make sure for a yellow transparent acidic TiO_2 sol. The sol was kept at room temperature for thirty min.

Second component of nanocomposites is ZnO. First, Zinc nitrate hexahydrate was dissolved in pure alcohol and was stirred for five min. Then the mixture of diethanol amine, pure alcohol, and deionized water was added to solution under vigorous constant stirring condition. The solution was constantly stirred for fifteen minutes to reach a transparent sol ZnO.

Third component of nanoparticle is CuO. To beginning, Copper (II) nitrate hexahydrate was dissolved in the pure alcohol and stirred for five minutes. Then, the mixture of ethanol amine, pure alcohol and distillated water was added to solution under vigorous constant mixing condition. The solution was steadily mixed for fifteen minutes to reach an alkalify transparent sol CuO.

Finally, the sol of ZnO, and CuO was mixed directly with the sol of TiO_2 to prepare the TiO_2-ZnO-CuO nanocomposite. That nanocomposite was dried at room temperature. Then, the nanocomposite sintered at the temperature of 350 °C for 10 min and after that, sintered at the temperature of 500 °C for five hours in order to calcinate (the temperature was being increased five Celsius per second) and finally, the catalyst was prepared [22]

Experimental

All photochemical reactions for destruction of MTBE with TiO_2-ZnO-CuO were fulfilled in a batch reactor made from cylindrical glass with three liter in volume. Reaction mixture in the reactor circulates in the closed cycle between pump and reactor. In addition, reactions' temperature was monitored. Three 15 W lamps from Phillips emitting UV light of wavelength 254 nm, which was immersed in the solution, was applied to serve the UV radiation in the reactor. The volume of the reaction mixture for each of the tests, which proposed by Response surface methodology (RSM) experimental design, was 3 L. In the end, The MTBE concentrations were measured with the device of UV-Vis spectrophotometer. A scheme of the reactor used in this study is represented in Figure 1.

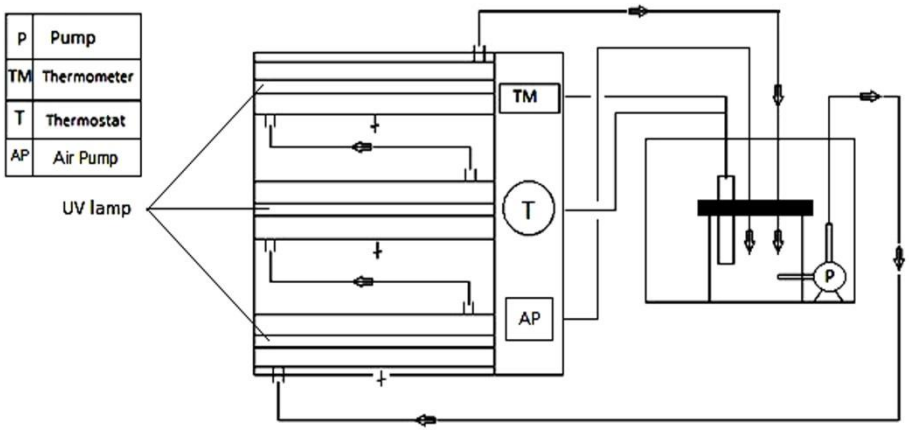

Figure 1. Scheme of the reactor used in this study is represented

Analysis

Methyl *tert*-butyl ether removal was evaluated by Gas Choromatography device. The percentage of MTBE removal was determined using Eq. (1).

$$\text{MTBE removal (\%)} = (C_0 - C_t)/ C_0 \times 100 \quad (1)$$

Where C_0 is the initial concentration of MTBE in ppm and C_t is MTBE's concentration based on ppm at any time t.

Experimental design and statistical analysis

Initially preliminary experiments were conducted using single factor study method to identify the significant experimental parameters affecting the photocatalytic MTBE treatment. The selected factors were catalytic dose, initial concentration of MTBE and pH of reaction mixture.

The three selected experimental parameters were optimized by RSM as the independent variables and the percentage of degradation of MTBE as the response variables. Box–Behnken design of experiments is employed to examine the combined effects of the three independent variables on the response through 15 sets of experiment. The ranges and levels of the independent variables are shown in Table 1. Box–Behnken design is applied because it is highly efficient and does not involve any point at the peaks of the cubic region formed by the variables' upper and lower limits.

Table 1. The levels and ranges of variables in Box–Behnken statistical experiment design

Independent variables	Symbol	Coded variable level		
		low	center	high
		-1	0	+1
pH	A	4	7	10
MTBE concentration (mg/L)	B	30	40	50
Catalytic loading (g/L)	C	1	2	3

This design along with RSM has been widely used to optimize various physical, chemical and biological processes [23-26]. By using RSM, the results are matched to an empirical quadratic polynomial model for the three parameters expressed in the equation 2:

$$Y=\beta_0+\beta_1A+\beta_2B+\beta_3C+\beta_4D+\beta_{11}A^2+\beta_{22}B^2+\beta_{33}C^2+\beta_{44}D^2+\beta_{12}AB+\beta_{23}BC+\beta_{31}CA+\beta_{14}AD+\beta_{24}BD+\beta_{34}CD \quad (2)$$

Where, Y denotes the response variable, β_0 the intercept, β_1, β_2, β_3 the coefficients of the independent variables, β_{11}, β_{22}, β_{33} quadratic coefficients, β_{12}, β_{23}, β_{31}, β_{14}, β_{24}, β_{34} the interaction coefficients and A, B, C are the independent variables. Multivariate regression analysis and optimization process were performed by means of RSM and using Design Expert software (version 7, Stat Ease Inc., USA). The obtained values from analysis of variance (ANOVA) were found significant at $P<0.05$. The optimum values for the independent variables were found using three-dimensional response surface analysis of the independent and dependent variables. The designed experiments and the experimental and predicted values of the response were detailed in Table 2 and Figure 2. The effect of the independents variable on the degradation of MTBE was shown in Figure 3 (a, b, c).

Table 2. Box–Behenken experiments along with actual and predicted values of responses

Run	A , pH	B , MTBE concentration (mg/L)	C , Catalyst loading (g/L)	MTBE removal (%)	
				Actual	Predicted
1	10	40	3	40.679	40.674
2	7	50	3	63.654	64.052
3	4	30	2	90.043	90.437
4	7	40	2	87.253	87.414
5	4	40	1	47.973	47.978
6	7	40	2	87.534	87.414
7	7	30	1	90.081	89.683
8	7	30	3	93.794	93.897
9	7	50	1	57.252	57.151
10	10	40	1	33.679	34.147
11	7	40	2	87.456	87.414
12	4	50	2	52.263	52.360
13	10	30	2	70.784	70.687
14	10	50	2	46.781	46.387
15	4	40	3	53.088	52.593

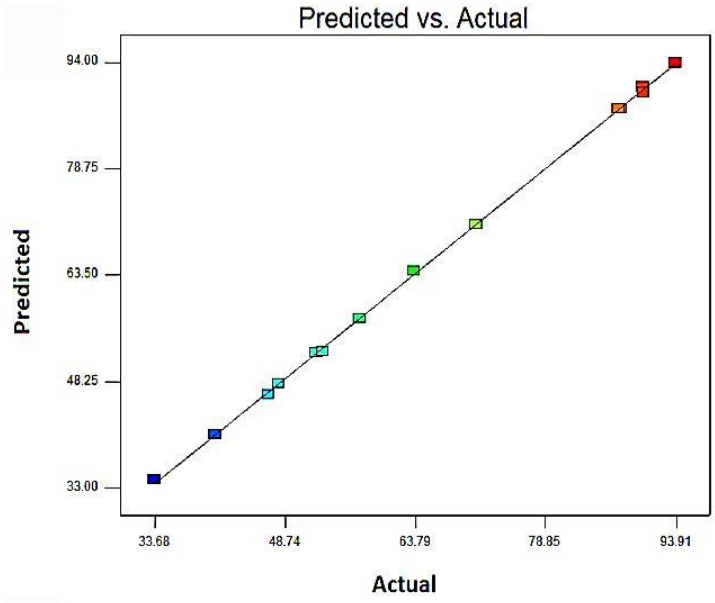

Figure 2. Plot of the actual and predicted values for degradation of MTBE

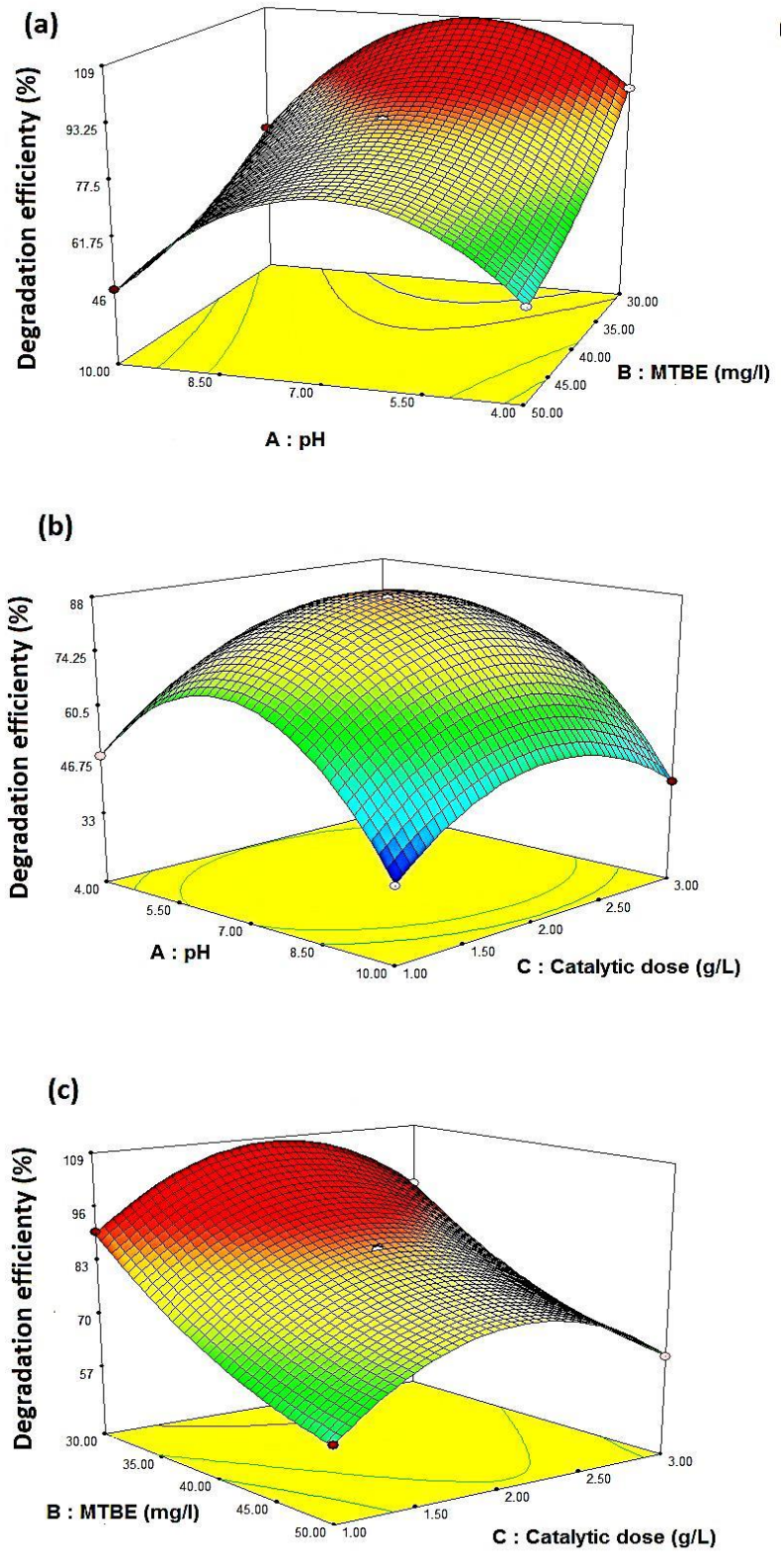

Figure 3. Surface plots of MTBE removal (%) in uncoded values for t = 60 min. (a) A (pH) and B (dye) in fixed C (catalyst concentration) at 2 g L^{-1}, (b) A (pH) and C (catalyst concentration) in fixed B (dye) at 40 mg L^{-1}, (c) B (dye) and C (catalyst concentration) in fixed A (pH) at 7.

RESULTS AND DISCUSSION

X-ray diffraction and SEM

The X-ray diffraction (XRD) was used to identify the structure of prepared TiO_2-ZnO-CuO and TiO_2 nano-particles, which were shown in Figure 4a. According to the Figure 4a, all peaks are found at 25.38º, 37.94º, 48.04º, 54.69º and 62.93º for TiO_2; and 25.32º, 37.63º, 48.06º, 54.58º and 62.91º for TiO_2-ZnO-CuO. The two Theta values of x-ray patterns of TiO_2 and TiO_2-ZnO-CuO are compatible with anatase for both of them. The XRD patterns illustrate that the composition of TiO_2-ZnO-CuO does not change the catalyst structure of TiO_2. This may result from the low concentration of CuO and ZnO in the composition was low. The particle size of the samples can be calculated by Debye-Scherrer formula:

$$D = \frac{K\lambda}{\beta \cos\theta} \qquad (3)$$

In Eq.3 , D is the average crystal size (nm), K is the Scherrer constant, a arbitrary value that falls within the range 0.8-1.0 (it is assumed to be 0.9 in the present study), λ is wavelength of X-ray radiation (0.154 nm) , θ is the diffraction angle and ß is full width at half maximum (FWHM). The particle size calculated value for TiO_2 and TiO_2-ZnO-CuO nanoparticles is 11.84 nm and 11.78 nm, respectively.

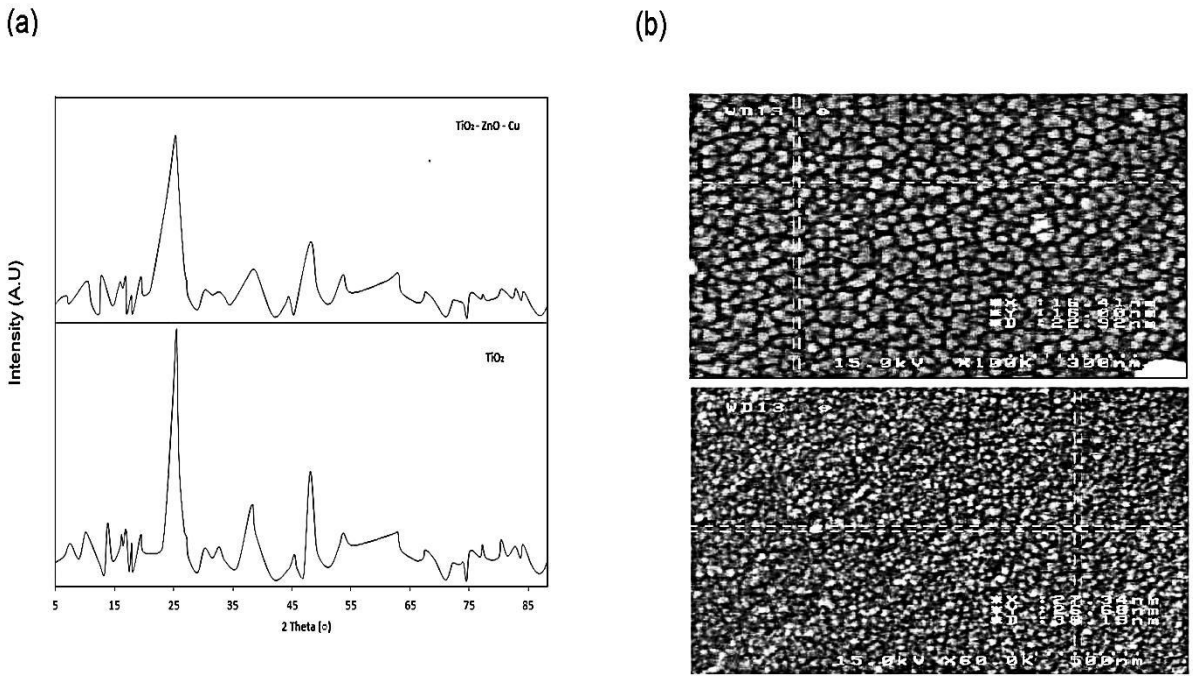

Figure 4. Catalyst characterization (a) XRD pattern of TiO_2 and TiO_2–ZnO-CuO, (b) SEM image of TiO_2–ZnO-CuO.

Scanning electron microscope (SEM) was applied to reveal the morphology of surface's samples, which were prepared in this work, which is shown in Figure 4b. This figure shows that sphere-shaped particles are formed in good resemblance to each other. Relying on the SEM Images, the average particle size of TiO_2-

ZnO-CuO nanoparticles is approximately 18.75 nm. Furthermore, there was a difference between crystal size evaluated by XRD and by SEM. This difference can be originated from this fact that the outcome of an XRD pattern reveals the crystal size of a particle, whereas the result of a SEM image represents the particle size itself, which is the accumulation of several crystals [27-29].

STATISTICAL ANALYSIS

To gain a suitable model, tests of significance for the regression model and for each coefficient of the model as well as the test for lack-of-fit ought to be conducted. ANOVA for the models was performed and the significance of model was examined by Fisher's statistical test (F-test) by testing the significant differences between sources of variation in experimental results, i.e., the significance of the regression, the lack of fit, and the coefficient of multiple determination (R^2) [30]. Since the full second-order models (models containing all two-parameter interactions) were not accepted by the mentioned tests, they were improved by elimination of the model terms until the determined conditions were fulfilled.

The R-square is 0.9998, which is close to 1 and significant, implying that about 99.98 % of changes in the data can be explained by the model. Adequate accuracy compares the range of the estimated value at design points with the mean prediction error. The ratios greater than 4 indicate the model's adequate discrimination power. The result of the above comparison is greater than 4, implying the model's adequate discrimination power. The lack-of-fit P- value of 0.0522 suggests the lack-of-fit is not significant relative to net error; this is suitable, since we look for a model that matches.

Following the experimental design (Table 2), empirical second order polynomial equations are developed for the percentage of degradation of MTBE in terms of the three independent variables as it is expressed in equation 4.

$$\text{MTBE removal} = 87.41 - 6.43\,A - 15.59\,B + 2.78\,C + 3.44\,AB + 0.47\,AC + 0.67\,BC - 27.39\,A^2 + 4.95\,B^2 - 16.17\,C^2 \quad (4)$$

The ANOVA of the second order polynomial model (F-value = 2843.13, *P*-value < 0.0001) shows that the model is significant, i.e. there is only a chance of 0.01% for occurrence of the model's F-value due to the noise. The ANOVA regarding the regression model's coefficient of degradation of MTBE is an extra tool to check the final model's adequacy. The normal probability plot (Scatter Diagram) for the studentized residuals is presented in Figure 5a The points on this plot lie reasonably close to the straight line, confirming that the errors have normal distribution with a zero mean and a constant. The curvature *P*-value< 0.0001 indicates that there is a significant curvature (as measured by the difference between the mean center points and the mean factorial points) in the design space. Consequently, a linear model along with the interaction terms giving a twisted plane was not adequate to explain the response. Likewise, plots of the residuals in Figure 5b reveal that they have no obvious pattern and their structure is rather abnormal. Moreover, they indicate equal scatter above and below the x-axis, implying the proposed model's adequacy, so there is no reason to suspect any violation. The optimum conditions for the maximum degradation of MTBE were shown in Table 3.

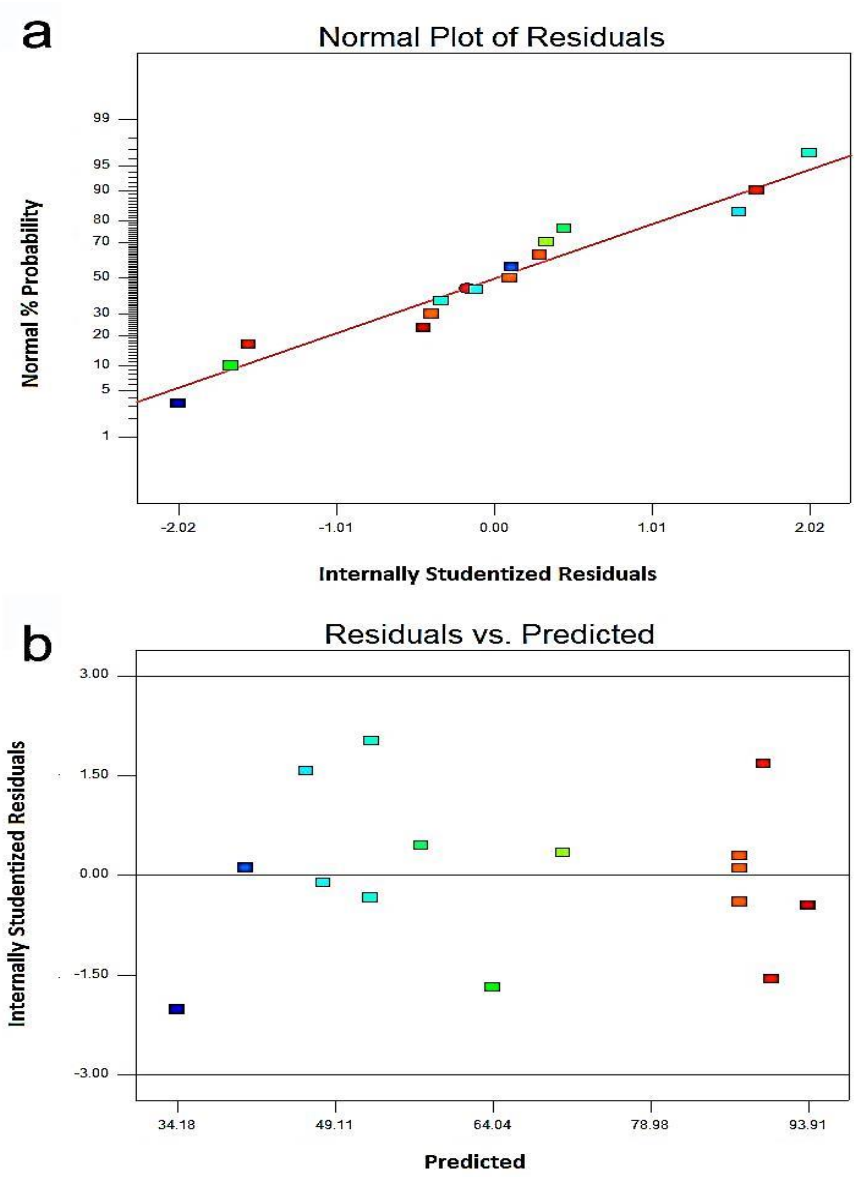

Figure 5. (a) Normal probability plot of residual for degradation efficiency %; (b) plot of residual and predicted values for degradation of MTBE

Table 3. The Optimum conditions selected for the maximum possible MTBE removal %

Num.	A, pH	B, initial MTBE Concentration (mg/L)	C, catalytic dose (g/L)	MTBE removal (%) (predict)	MTBE removal (%)(actual)	Desirability
10	7	31.46	1.49	99.0489	95.6372	1

Effect of Initial pH on the photocatalysis of MTBE

One of the most significant variables in photocatalytic degradation of organic contaminants is pH. The impacts of pH on the photocatalytic degradation of MTBE were assessed with the initial pH at three diverse values of 4, 7 and 10, as it is illustrated in Figure 6a. The destruction of MTBE goes down as the

pH of solution increases from 4 to 7. Then, the percentage of MTBE degradation goes up where as solution's pH value raises from 7 to 10. The pH of the solution has sophisticated effects on the photocatalytic oxidation reaction. Generally, the pH effect depends on the type of pollution and zero point charge (ZPC) of semiconductor (catalyst) in the oxidation process. The phenomenon can be represented in terms of the location of the point of zero charge (isoelectric point) of the TiO_2-ZnO-CuO. The best pH value for degradation of MTBE under mentioned condition is 7 (Figure 3). Similar results have been reported for the photocatalytic oxidation [21, 29].

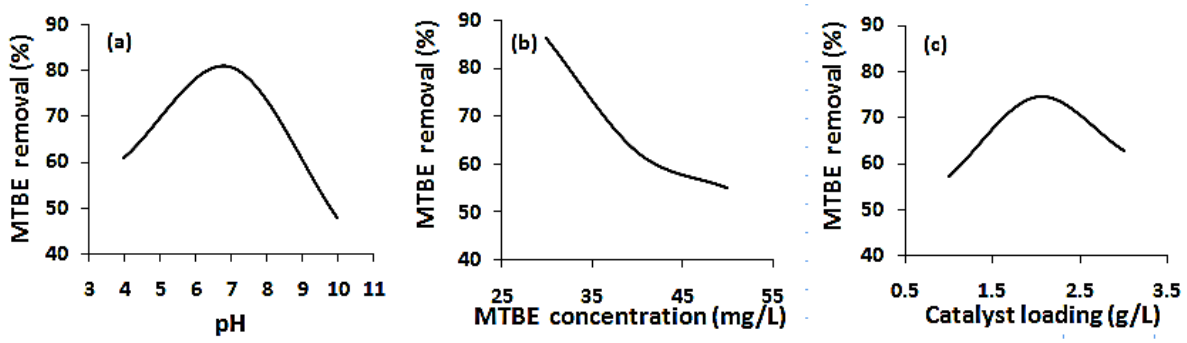

Figure 6. Effect of pH, initial MTBE concentration and catalytic dose on degradation efficiency %: (a) initial MTBE concentration: 40 (mg/L); catalytic dose: 2 (g/L), (b) pH: 7; catalytic dose: 2 (g/L), (c) pH: 7; initial MTBE concentration: 40 (mg/L).

Effect of TiO_2 – ZnO-CuO concentration on photocatalysis of MTBE

The experiments were performed to investigate the influence of catalyst loading on photocatalytic degradation MTBE under conditions 1, 2 and 3g/L of catalyst loading. Figure 6b shows the percentage of degradation efficacy versus catalyst loading for several initial TiO_2-ZnO-CuO nonoparticles' concentrations. According to the Figure 6b, it is clear that the percentage of degradation efficiency rises as the catalyst loading raises from1 to 3 g/L. However, this trend reverses and the percentage of degradation MTBE goes down as catalyst loading is increased from 1 to 2 g/L. As the amount of catalyst increases, the number of adsorbed photons and molecules raise as well due to grow in the number of TiO_2-ZnO-CuO nanoparticles. As a result, the particles' density within the illumination area increases. [31] This behavior can be attributed that some photocatalyst particles may not get sufficient energy to produce hydroxyl radical and start MTBE oxidation [23]. It may also result from TiO_2-ZnO-CuO aggregation, increasing obscurity, reducing the active points on its surface to adsorb organic compounds and UV, thereby reducing the quantity of e-h+ and OH free radicals and affecting the degradation [23, 26].

Effect of initial concentration of MTBE on degradation of MTBE

In this section the effect of various initial concentrations of MTBE solution on degradation of MTBE was experimented, which results of this test was shown in Figure 6c. Based on the Figure 6c, it is clear that increasing of initial concentration of MTBE leads to less degradation of MTBE. Similar results have been reported on the photocatalytic oxidation of other organic compounds interface [2, 23, 29, and 32]. Thus, at low concentration of MTBE, a rapid degradation MTBE

results from a larger number of water molecules that will be adsorbed onto the available TiO_2-ZnO-CuO particles, producing hydroxyl radicals. On the other hand, at high concentration of MTBE, there is a smaller portion of water molecules to free active sites, since the number of active sites remains the same. As a result, it intensifies the competition between the MTBE and water molecules to adsorb on catalyst, causing to drop in the degradation rate.

Effect of optimized conditions on removal of MTBE

Kinetics of photocatalytic degradation of the MTBE was evaluated based on optimum conditions obtained from previous sections, which is shown in Figure 7 at catalyst concentration 1.49 g/L, pH = 7 , initial MTBE Concentration 31.46 (mg/L), and under light intensity 15 W UV-C. Generally, first-order kinetics is suitable for photocatalytic reactions [2, 17]. Kinetics model as follows:

$$-r_A = -\frac{dC}{dt} = KC \qquad (5)$$

After integration of Eq. (6), the following equation is obtained:

$$Ln\left(\frac{C_0}{C}\right) = K\,t \qquad (6)$$

Where r_A is the oxidation rate of the MTBE (ppm min^{-1}), K the apparent constant of the reaction rate (the constant of first order reaction), C the concentration of the MTBE (ppm), C_0 the initial concentration of MTBE, t the time required for the initial concentration of MTBE C_0 to become C (min).

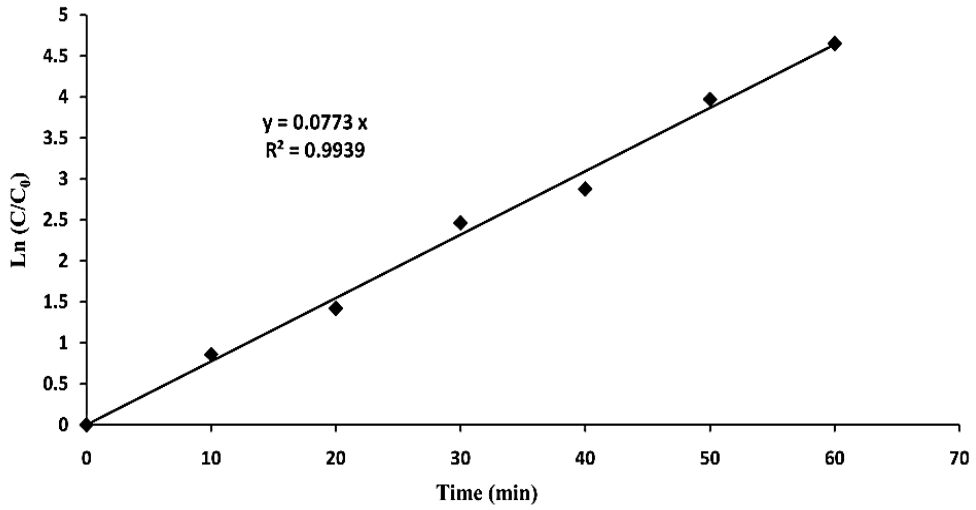

Figure7. Effect of different initial concentrations of the MTBE on photocatalytic degradation based on optimum conditions

The slope of the Ln (C_0/C) versus time plots under optimized conditions represents the Rate constant of degradation MTBE. Values of the first-order degradation constants (K) as well as the linear regression (R^2) values are reported in Table 4.

Table 4. Optimum conditions and Kinetic constant of MTBE degradation

Num.	A, pH	B, initial MTBE Concentration (mg/L)	C, catalytic dose (g/L)	R^2	$K_{app}(min^{-1})$
10	7	31.46	1.49	0.9939	0.0773

CONCLUSIONS

In this study, the sol−gel method was applied to synthesize TiO_2- ZnO-CuO nanoparticles as the catalyst to degrade MTBE solution by photocatalytic method. The crystal size of TiO_2- ZnO-CuO is 11.78 nm that is evaluated by Debye-Scherrer formula. The XRD data showed that the prepared nanoparticles had the same crystals structures as the pure TiO_2. The optimization and the modeling of photocatalytic degradation of MTBE were performed by using a composite experimental design. The ensuing mathematical model could predict the photocatalytic degradation at any point in the experimental domain as well as the determination of the optimal degradation conditions. Under optimized conditions, the experimental values agreed with the values predicted by the ridge analysis. These results implicate that the optimization using a response surface methodology based on the Box- Behnken design can save the time and effort by the estimation of the optimum conditions of the maximum removal of MTBE. In addition, the optimal vital operation parameters are found by RSM method at pH of 7, TiO_2-ZnO-CuO concentration of 1.49 g/L, and an initial concentration of MTBE 31.46 mg/L. Under the optimum conditions, performance of photocatalytic degradation reaches 99.0489 % in 1 hour. While Hu et al. [2] indicated that under the optimal conditions (initial MTBE concentration of 1mM were acidic and 15mM H_2O_2 in UV/H_2O_2 system, and pH 3.0 and 2.0 g/l TiO_2 in UV/TiO_2 suspended slurries system), MTBE photodegradation during the initial period of 1 hour in UV/H_2O_2 and UV/TiO_2 systems reached 98 and 80%, respectively. The Rate constant of degradation MTBE under optimum condition was 0.0773 K_{app} (min^{-1}).

ACKNOWLEDGEMENTS

The authors wish to thank the Ilam University, Iran for financial support.

REFRENCES

1. Zang Y., Farnood R., 2005. Photocatalytic decomposition of methyl tert-butyl ether in aqueous slurry of titanium dioxide. Appl Catal. B. 57, 275–282.

2. Hu Q., Zhang C., Wang Z., Chen Y., Mao K., Zhang, X., Zhu M., 2008. Photodegradation of methyl tert-butyl ether (MTBE) by UV/H_2O_2 and UV/TiO_2. J Hazard Mater. 154, 795–803.

3. Pontius F.W., 1998. New Horizons in Federal Regulation. J Am Water Works Assoc. 90, 38-50.

4. Kuburovic N., Todorovic M., Raicevic V., Orlovic A., Jovanovic L., Nikolic J., Solevic T., 2007. Removal of methyl tertiary butyl ether from wastewaters using photolytic, photocatalytic and microbiological degradation processes. Desal. 213, 123-128.

5. Ahmed F.E., 2001. Toxicology and human health effects following exposure to oxygenated or reformulated gasline. Toxicol Lett. 123, 89-113.

6. François A., Mathis H., Godefroy D., Piveteau P., Fayolle F., Monot F., 2002. Biodegradation of MTBE and other fuel oxygenates by a new strain mycobacterum austroafricanum Ifp 2012. Appl Environ Microbiol. 68, 2754-2762.

7. Ji B.Y., Shao F., Hu G.J., Zheng S.R., Zhang Q.M., Xu Z.Y., 2009. Adsorption of methyl tert-butyl ether (MTBE) from aqueous solution by porous polymeric adsorbents. J Hazard Mater. 161, 81–87

8. Rossner A., Knappe D.R.U., 2008. MTBE adsorption on alternative adsorbents and packed bed adsorber performance. Water Res. 42, 2287–2299.

9. Squillace P.J., Pankow J.F., Korte N.E., Zogorski J.S., 1997. Review of the environmental behavior and fate of methyl tert-butyl ether. Environ Toxicol Chem. 16, 1836–1844.

10. Fiorenza S., Rifai H.S., 2003. Review of MTBE biodegradation and bioremediation Biorem J. 7, 1–35.

11. Cater S.R., Dussert B.W., Megonnell N., 2000.

Reducing the threat of MTBE-contaminated groundwater. Pollut Eng. 32, 36–39.

12. Salari D., Niaei A., Khataee A., Zarei M., 2009. Electrochemical treatment of dye solution containing C.I. Basic Yellow 2 by the peroxi-coagulation method and modeling of experimental results by artificial neural networks. J Electroanal Chem. 629, 117-125.

13. Khataee A.R., Zarei M., Moradkhannejad L., 2010. Application of response surface methodology for optimization of azo dye removal by oxalate catalyzed photoelectro-Fenton process using carbon nanotube-PTFE cathode. Desalination. 258, 112-119.

14. Khataee A.R., Zarei M., Fathinia M., Khobnasab Jafari M., 2011. Photocatalytic degradation of an anthraquinone dye on immobilized TiO_2 nanoparticles in a rectangular reactor: Destruction pathway and response surface approach. Desalination. 268, 126-133.

15. Daneshvar N., Aber S., Seyed Dorraji M.S., Khataee A.R., Rasoulifard M.H., 2007. Photocatalytic degradation of the insecticide diazinon in the presence of prepared nanocrystalline ZnO powders under irradiation of UV-C light. Sep Purif Technol. 58, 91-98.

16. Khodja A.A., Sehili T., Pilichowski J.F., Boule P., 2001. Photocatalytic degradation of 2-phenylphenol on TiO_2 and ZnO in aqueous suspensions. J Photochem Photobiol A Chem. 141, 231-239.

17. Colon G., Maicu M., Hidalgo M.S., Navio J. A., 2006. Cu-doped TiO_2 systems with improved photocatalytic activity. Appl Catal B. 67, 41–51.

18. Liqiang J., Honggang F., Baiqi W., Dejun W., Baifu X., Shudan L., Jiazhong S., 2006. Effects of Sn dopant on the photoinduced charge property and photocatalytic activity of TiO_2 nanoparticles. Appl Catal B. 62, 282–291.

19. Chang S.M., Doong R.A., 2006. Characterization of Zr-Doped TiO_2 nanocrystals prepared by a nonhydrolytic sol-gel method at high temperatures. J Phys Chem B. 110, 20808–20814.

20. Luo H., Takata T., Lee Y., Zhao J., Domen K., Yan Y., 2004. Photocatalytic activity enhancing for titanium dioxide by Co-doping with bromine and chlorine. Chem Mater. 16, 846-849.

21. Safari M., Nikazar M., dadvar M., 2013. Photocatalytic degradation of methyl tert-butyl ether (MTBE) by Fe-TiO_2 nanoparticles. J Ind Eng Chem. 19, 1697–1702.

22. Pirkarami A., Olya M.E., Farshid S.R., 2013. UV/Ni–TiO_2 nanocatalyst for electrochemical. Water Resour Industry. 5, 9-20.

23. Zhang J., Fu D., Xu Y., Liu C., 2010. Optimization of parameters on photocatalytic degradation of chloramphenicol using TiO_2 as photocatalyist by response surface methodology. J Environ Sci. 22, 1281-1289.

24. Ferreira S.C., Bruns R.E., Ferreira H.S., Matos G.D., David J.M., Brandao G.C., Dos Santos, W.N.L., 2007. Box-Behnken design: an alternative for the optimization of analytical methods. Anal Chim Acta. 597, 179–186.

25. Ay F., Catalkaya E.C., Kargi F., 2009. A statistical experiment design approach for advanced oxidation of Direct Red azo-dye by photo-Fenton treatment. J Hazard Mater. 162, 230-236.

26. Wang J.P., Chen Y.Z., Wang Y., Yuan S.J., Yu, H.Q., 2011. Optimization of the coagulation-flocculation process for pulp mill wastewater treatment using a combination of uniform design and response surface methodology. Water Res. 45, 5633–5640.

27. Zhou M., Yu J., Cheng B., 2006. Effects of Fe-doping on the photocatalytic activity of mesoporous TiO_2 powders prepared by an ultrasonic method. J Hazard Mater. 137, 1838-1847.

28. Garcia J.C., Takashima K., 2003. Photocatalytic degradation of imazaquin in an aqueous suspension of titanium dioxide. J Photochem Photobiol A Chem. 155, 215-222.

29. Eslami A., Nasseri S., Yadollahi B., Mesdaghinia A., Vaezi F., Nabizadeh R., Nazmara S., 2008. Photocatalytic degradation of methyl tert-butyl ether

(MTBE) in contaminated water by ZnO nanoparticles. J Chemical Technol Biotechnol. 83, 1447-1453.

30. Myers R.H., Montgomery D.C., 2002. Response surface methodology: process and product optimization using designed experiments. Second ed., Wiley, NewYork.

31. Nikazar M., Gholivand K., Mahanpoor K.,2008. Photocatalytic degradation of azo dye Acid Red 114 in water with TiO_2 supported on clinoptilolite as a catalyst. Desal. 219, 293-300.

32. Tonga T., Zhanga J., Tiana B., Chena F., Heb D., 2008. Preparation of Fe^{3+}-doped TiO_2 catalysts by controlled hydrolysis of titanium alkoxide and study on their photocatalyticactivity for methyl orange degradation. J Hazard Mater. 155, 572-579.